Green Chemistry

Accepted Manuscript

Green Chemistry

Cutting-edge research for a greener sustainable future
www.rsc.org/greenchem

Volume 18 | Number 7 | 7 April 2016 | Pages 1821–2242

ISSN 1463-9262

ROYAL SOCIETY OF CHEMISTRY

CRITICAL REVIEW
G. Chatel et al.
Heterogeneous catalytic oxidation for lignin valorization into valuable chemicals: what results? What limitations? What trends?

175 YEARS

ROYAL SOCIETY OF CHEMISTRY

rsc.li/green-chem

ROYAL SOCIETY
OF CHEMISTRY

Green Chemistry

ARTICLE

Aqueous phase reforming of glycerol using doped graphenes as metal-free catalysts

Iván Esteve-Adell,[a] Bertrand Crapart,[a,b] Ana Primo,[a] Philippe Serp[b] and Hermenegildo Garcia [a,*]

Boron-doped graphene obtained by pyrolysis at 900 ^{o}C of the boric acid ester of alginate was found the most active graphene among a series of doped and co-doped graphenes to promote the aqueous phase reforming of glycerol at 250 ^{o}C. This reaction is of interest in the context of valorization of aqueous wastes of carbohydrate syrups. Control experiments adding to undoped graphene 1 wt. % of triphenylborane, tris(pentafluorophenyl)borane or bis(pinacolyl)diborane as models of possible boron atom types present in B-doped graphene, and boric acid that could be present in a residual amount after pyrolysis, show in all cases an increase in the catalytic activity of graphene. B-doped graphene has also activity for glucose aqueous phase reforming. B-doped graphene undergoes deactivation upon reuse, probably due to B leaching. The results show that graphenes are promising metal-free catalysts for aqueous phase reforming alternative to those containing platinum.

Introduction

In the context of biomass valorisation one of the reactions that has been considered as having large interest is the aqueous phase reforming (APR) of aqueous wastes containing sugar syrups.[1] These residues are generated during hydrolysis of cellulose, hemicellulose and other components of biomass. In APR, these aqueous wastes containing complex mixtures of carbohydrates can be used to generate additional amounts of H_2 that can be considered as derived from renewable and sustainable sources.[1, 2]

One of the current limitations of APR is the development of suitable catalysts for these processes. At the moment most of the efficient APR catalysts are based on platinum or its alloys and it would be highly desirable to develop more affordable alternative catalysts.[3-5] Looking for alternatives to expensive noble metals, there is much current interest in exploiting the possibilities of graphenes (Gs) as metal free catalysts.[6-8] Gs when obtained from biomass can be considered as sustainable catalysts.[9, 10] There is ample literature data showing that defective or doped Gs can exhibit catalytic activity for aerobic oxidations[11-13] and reductions including hydrogenation of C-C

multiple bonds[14, 15] and nitro groups.[14, 15]

Gs are particularly suitable as catalysts for biomass transformations since in this case Gs do not need to be removed from the reaction mixture after the reaction and do not introduce metallic impurities in the final residues. Continuing with this research line of using Gs as metal free catalysts,[16] in the present manuscript it will be reported that B-doped Gs are suitable metal-free catalysts to promote the APR of glycerol. Besides valorisation of glycerol formed in large amounts as by-product in biodiesel production,[17] APR of glycerol is considered a model reaction to evaluate the activity APR catalysts in complex carbohydrate syrups.[18]

Results and discussion

The reactions were carried out in autoclave at 250 ^{o}C under autogenous pressure using aqueous glycerol solutions (10 wt. %) as feed. As carbocatalysts a series of Gs with and without doping were evaluated. Table 1 lists the series of materials tested as well as their origin, preparation procedure and their main analytical data. The series of catalysts includes GO obtained from graphite after Hummers oxidation and exfoliation.[19, 20] However, most of the Gs were obtained by pyrolysis at 900 ^{o}C under inert atmosphere of alginate or chitosan without or after formation of the corresponding borates or phosphate esters[9, 10, 13, 21]. The presence of boric or phosphoric esters in the biopolymer determines that a fraction of these elements can become incorporated as dopant in the resulting G after the pyrolysis as it has been already reported in the literature.[13, 21]

[a.] Instituto Universitario de Tecnología Química, Universitat Politècnica de València-Consejo Superior de Investigaciones Científicas, Avenida de los Naranjos s/n, 46022 Valencia, Spain. E-mail: hgarcia@qim.upv.es.
[b.] CNRS, LCC (Laboratoire de Chimie de Coordination), composante ENSIACET, 4 allée Emile Monso, BP 44099, F-31030 Toulouse Cedex 4, France

**ARTICLE**

Scheme 1 illustrates the preparation procedure of the samples under study, while the heteroatom content is provided in Table 1. The purpose of having selected these materials is to

Table 1. List, preparation procedure and analytical data of G catalysts used in the present study.

Material	Method	Precursors	Element content (%)		
			Heteroatom	C	O
G	Pyrolysis 900 ^{o}C	Alginate	-	88.2	8.2
GO	Hummers	Graphite	-	47.3	48.9
(B)G	Pyrolysis 900 ^{o}C	Alginate + HBO$_3$	1.2	76.4	10.2
(N)G	Pyrolysis 900 ^{o}C	Chitosan	7.6	79.6	9.2
(P)G	Pyrolysis 900 ^{o}C	Alginate + NaH$_2$PO$_4$	2.6	77.5	9.3
(B,N)G	Pyrolysis 900 ^{o}C	Chitosan + HBO$_3$	2.1(B)/9.4(N)	62.7	9
(B,P)G	Pyrolysis 900 ^{o}C	Alginate + HBO$_3$ + NaH$_2$PO$_4$	0.9(B)/2.6(P)	71.5	9.8
MWCN	Commercial	-	-	95.4	4.1
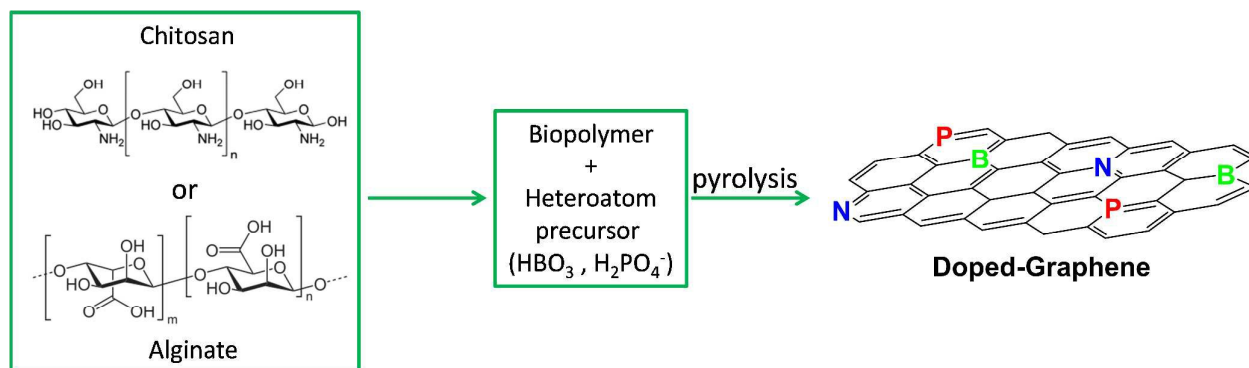
Scheme 1. Preparation procedure of doped Gs by pyrolysis of natural polysaccharides without or with esterification with inorganic acids.

establish the activity of Gs as catalysts of APR of glycerol and the influence of doping or co-doping on their APR activity.

All the materials screened in the present study as carbocatalysts for APR of glycerol have been previously reported and the properties of these samples are in good agreement with those in the literature.[13, 14] Specifically the graphenic structure having carbon vacancies and oxygenated functional groups can be assessed by Raman spectroscopy, monitoring the relative intensity of the G vs the D band that for the series of samples under study is always close to 1.15 % (Figure S1). This I_G/I_D value corresponds in general to G materials having defects associated to the presence of oxygenated functional groups, heteroatoms, carbon vacancies and holes. The 2D morphology of the samples can be evidenced by the TEM images of exfoliated materials, while HRTEM shows the hexagonal arrangement of the atoms (Figure S2). The single and few layers morphology of the G samples can be proved by AFM measurements of the thickness of the G sheets on atomically flat surfaces (Figure S3). The presence of the corresponding heteroatoms, their percentage and distribution among possible different structures is determined by combustion chemical analysis and XPS. Thus, in the case of G the presence of a residual oxygen content about 8 wt. % was determined. In the case of (N)G, two main families of N atoms (7.6 wt. % in total) namely graphenic and pyridinic N atoms with a relative percentage of 35 and 62.2 % was established (see Figure S4 in supplementary information). In the case (B)G also two populations of B atoms corresponding

to graphenic (BCCC) or B atoms bonded to oxygen (BCOO) with a percentage 54.8 and 45.2 %, respectively, was determined based on the values of the binding energies for these individual components.[22, 23] The high oxophilicity of boron atoms determines that even under the strong reducing conditions of the pyrolysis, favouring the formation of dopant element-C bonds and their incorporation in the lattice, the largest population of B atoms still are bonded to oxygen with a BCCO environment according to deconvolution of the B1s peak in high resolution XPS (see Figure S5 in supplementary information). It should be commented that this assignment of B atom types is based on the literature data,[22, 23] but, as it will be commented later when discussing the leaching of B atoms, it could be this assignment and the relative percentages is not correct in the present case, due to specific interactions of B species with the graphenic structure. Table 1 summarises the heteroatom content for the rest of carbocatalysts of the series.

Catalytic activity for APR of glycerol

A possible stoichiometry for complete APR mineralization of glycerol is indicated in Eq. (1). As it can be seen there for this ideal stoichiometry, 1 mol of glycerol can form up to 7 mols of H$_2$ and 3 of CO$_2$. It is, however, possible that other transformations of glycerol not resulting in complete mineralization render other products as well as H$_2$ and CO$_2$, although in lower proportions than in the complete mineralization.

$$C_3H_8O_3 + 3\ H_2O \rightarrow 7\ H_2 + 3\ CO_2 \qquad \text{Eq. (1)}$$
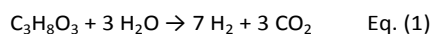
Preliminary controls of APR of glycerol in the absence of any catalyst or treating G catalyst suspended in pure water without any glycerol showed that H_2 and CO_2 formation is considerably much lower than the values of H_2 and CO_2 evolution when
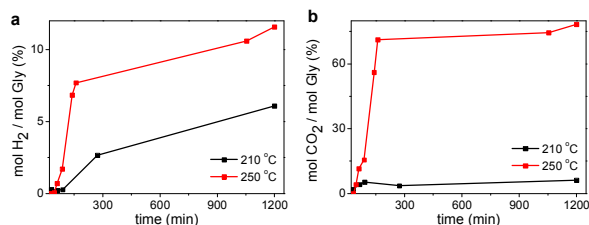

Figure 1. Time conversion plots for H_2 (a) and CO_2 (b) evolution in the APR reaction of glycerol promoted by G. Reaction conditions: Glycerol 10 vol. %, G 10 wt. % respect to glycerol, temperature 210 (black lines) or 250 (red lines) ^oC.

both glycerol (10 vol. %) or the carbocatalyst (20 wt. % respect glycerol) are simultaneously present.

It was observed that an increase on the reaction temperature in the range 200-250 ^oC favours notably the APR reaction of glycerol. As an example Figure 1 shows the temporal evolution of H_2 and CO_2 at 210 and 250 ^oC using G as catalyst. Other products observed in the gas phase with much lesser concentration are methane and ethane accompanied by trace amount of propane.

Accordingly 250 ^oC that was about the maximum temperature of our setup was selected as a suitable temperature for further studies. Perusal of Figure 1 and comparison with the ideal stoichiometry indicated in Eq. (1) show that the amount of CO_2 evolved in the reaction is much higher than that expected in view of the amount of the H_2. It has to be reminded that the origin of this higher-than-expected amount of CO_2 cannot be G since, as commented earlier, in the absence of glycerol the evolution of CO_2 from G under the same conditions is negligible (0.36 mmol). It is more probable that H_2 and CO_2 are

derived from glycerol through other reactions different than that corresponding to the complete mineralization of CO_2.

The amount of catalyst for achieving optimal APR reaction was studied in the range from 10 to 20 wt. % respect to glycerol, whereby it was observed that H_2 and CO_2 evolution increases with the amount of G present and, therefore, 20 wt. % was considered the most convenient catalyst loading reaching a compromise between amount of catalyst and H_2 production (Figure S6). It should be commented that these percentages of G with respect to substrate, and even higher, are common in the use of G as carbocatalysts.[11, 24, 25] Also this range of catalyst to substrate weight percentages is not unreasonable considering that G can be derived from biomass residues and it can be more affordable than precious metals.

With the optimal conditions of temperature and amount of catalyst the APR reaction of glycerol was screened with the series of carbocatalysts. Figure 2 shows the temporal profiles of H_2 and CO_2 generation promoted by the series of carbocatalysts under study showing the remarkable influence of doping on the catalytic activity. It was observed that GO and (N)G were completely inefficient to promote the reaction. Also the activity of (P)G was very low. In contrast, the activity of G increases significantly upon boron doping, (B)G and (B,N)G being the two most active samples (see Figure 2 and Figure S7). In the present study it is assumed that Gs are completely dispersed in the aqueous phase as single sheet with similar surface area. Unfortunately, BET measurements on dry powders are meaningless to support this assumption since the conditions of the isothermal gas adsorption measurements do not allow exfoliation of the G samples. Accordingly it is proposed that the different catalytic activity observed for the set of G samples arises from heteroatom doping. There are abundant precedents showing that the presence of heteroatoms can play a remarkable role on the catalytic activity and the data shown in Figure 2 would constitute another example.[6]
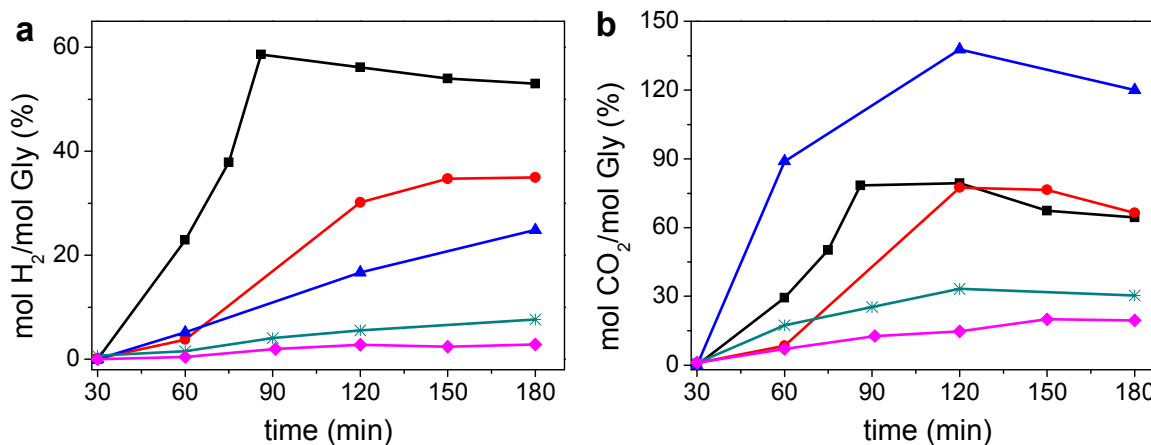

Figure 2. Temporal profile of H_2 (a) and CO_2 (b) evolution in the presence of a series of doped G as catalysts. (■) (B)G, (●) (B,N)G, (▲) G, ( ) (P)G, (♦) (N)G. Reaction conditions: Glycerol 10 vol. %, catalyst 20 wt. % respect to glycerol, temperature 250 ^oC.

Journal Name ARTICLE

In the case of the most efficient carbocatalysts, the temporal profile of H_2 and CO_2 evolution shows a maximum value, decreasing the amount of H_2 and CO_2 for longer reaction times. This decrease in H_2 and CO_2 is accompanied by a concomitant increase in the concentration of methane and other light alkanes in the gas phase. Therefore, the kinetic data indicate the occurrence of CO_2 methanation (Eq. 2) in a certain extent.

$$CO_2 + 4 H_2 \rightarrow CH_4 + 2 H_2O \quad (Eq. 2)$$
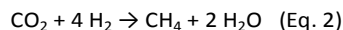
Thus, as the concentration of H_2 and CO_2 grows in the gas phase, the reaction between these two molecules would form methane and other by-products. This methanation should also be catalysed by (B)G, since it is known that CO_2 methanation is a catalytic process that does not occur at significant rates below 450 ^{o}C in the absence of catalyst.[26] It should be, however, commented that the "exact" stoichiometry predicted for equation 2 is, again, not experimentally observed, indicating that besides methanation, confirmed by formation of CH_4, other processes including hydrocarbon formation and generation of other products, should also be taking place simultaneously, resulting in a complex array of processes occurring at expense of the evolved H_2 and CO_2. It should be noted that, besides methane, ethane, ethylene and propane are also detected in the gas phase.

Figure 2 also presents the CO_2 evolution. It was observed that most of the doped G also evolved CO_2, although in much lower amounts than those measured when undoped G was used as catalyst. Thus, the samples containing boron as dopant element were the ones producing the highest amounts of H_2 with a H_2/CO_2 mol ratio higher than that of G. However in spite of the more favourable H_2/CO_2 molar ratio the value obtained for (B)G, about 1, is still lower than that expected for complete mineralization of glycerol corresponding to Eq. (1).

To put the catalytic activity of (B)G into context, APR of glycerol was also carried out under the optimal conditions using Pt(3wt.%)/C as a reference catalyst using Pt/Gly mol ratio of 0.5 %. The results obtained (see Figure S8 in Supplementary information) for the temporal evolution of H_2 shows that the catalyst containing Pt was, under the above conditions, far more active than (B)G, exhibiting an initial reaction rate of 470 mol h^{-1} compared to 54 mol h^{-1} measured for (B)G. Also, the maximum mol H_2/mol Gly value achieved for Pt/C was 415 % at 4 h that is significantly higher than 58 % reached for (B)G at 1.5 h. It is, therefore, clear that the performance of (B)G is about 1 order of magnitude lower than that reached with Pt as catalyst under the Pt/Gly used in these measurements. It should be, however, commented that other reported transition metal catalysts such as nickel are also significantly much less active than Pt and have catalytic activity in the same range as (B)G[3, 27].

With the best performing APR catalyst, an additional reaction using glucose as substrate was carried out. It is known in literature that the difficulty of APR, using metal catalyst such as Pt, increases along the number of C atoms of the polyol and the complexity of the saccharide mixture.[1, 28] A similar trend was also observed using (B)G as catalyst. As it can be seen in Figure 3, although (B)G was also able to promote the evolution

of the H_2 and CO_2 from glucose under the optimal conditions found for glycerol, the amount of H_2 was significantly lower than that obtained using glycerol as starting material.

Catalyst stability.

Stability of (B)G as APR catalyst was determined by performing five consecutive uses and by characterizing the used catalyst. Figure 4 presents the temporal profiles of (B)G as APR catalyst upon reuse. As it can be seen there, not only the H_2 production at 6 h reaction decreases upon reuse, but also the initial reaction rates, indicating that (B)G undergoes deactivation under the conditions of the APR.
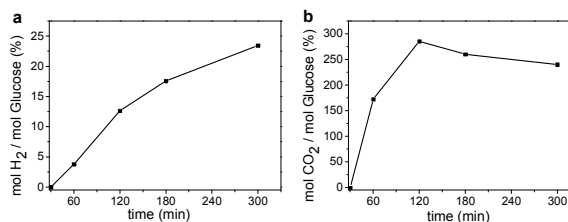

Figure 3. Time conversion plots for H_2 (a) and CO_2 (b) evolution in the APR reaction of glucose promoted by (B)G. Reaction conditions: Glucose (1.74 mmol) (B)G 20 wt. % respect to glucose, temperature 250 ^{o}C.
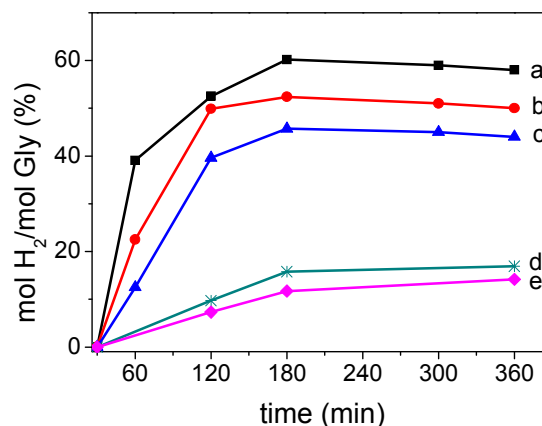

Figure 4. Temporal profile for H_2 evolution for the first (a), second (b), third (c), fourth (d) and fifth (e) use of (B)G in the APR reaction of glycerol promoted. Reaction conditions: Glycerol 10 vol.% (B)G 20 wt. % respect to glycerol, temperature 250 ^{o}C.

To understand the reasons for (B)G deactivation, characterization of the used catalyst was performed by Raman and XP spectroscopies and by TEM. No change in the Raman spectra of the (B)G sample before and after five uses of the material was observed (Figure S9), suggesting that no further defects on the G sheet have been produced under the APR conditions in an extent sufficient to be detectable by this spectroscopy. XPS of the five times used (B)G sample showed that while the C1s peak does not undergo significant changes (Figure S10), the B peak has completely disappear and the

ARTICLE
Journal Name

presence of B becomes undetectable by XPS. This leaching of B atoms appears to be in contradiction with the previous deconvolution of the B1s peak of fresh (B)G that agrees with the grafting of B on the G sheet, as reported previously.[13, 22, 23] However, it should be noted that the temperature and conditions of APR (high concentrations of carboxylic acids in H_2O) are favourable for dopant leaching.

TEM images of the used catalyst shows that the 2D morphology of (B)G is still preserved after the reaction. Figure S11 in the supplementary information presents a set of images taken for used (B)G at different magnifications and in different parts of the sample. In view of the available data showing that the properties of (B)G and its composition, it is suggested that the main cause of deactivation is the loss of boron doping taking place during the APR.[14] It should be noted that in related precedents it was observed that treatment of doped Gs with H_2 causes detachment of the dopant elements from the G sheet.[14]

To compare the stability of B on G with other related boronated organic molecules, BPh_3 was submitted to hydrothermal treatment at 250 oC in autoclave. ^{11}B NMR spectra of the aqueous solution before and after treatment compared to that of boric acid is presented in Fig. S12 of the supporting information. It was observed that after 6 h of hydrothermal treatment of BPh_3 is converted into boric acid, indicating that the conditions of APR can produce hydrothermal B-C bond cleavage and the occurrence of this process can explain the detachment of B from the graphene sheet.

Mechanistic studies

To gain some understanding on the activity data shown in Figure 2 and the positive influence of boron-doping, four experiments in where four boron-containing molecules added on purpose to undoped G were carried out. Specifically in these experiments the molecules selected were triphenylborane and tris(pentafluorophenyl)borane that can be considered models of graphenic boron (BCCC), bis(pinacolyl)diborane (BOO), having two neighbour boron atoms bonded to oxygen, and boric acid that could be present in a residual amount after pyrolysis. Specifically in the case of tris(pentafluorophenyl)borane and bis(pinacolyl)diborane, these two molecules were selected to favour their adsorption on G and their insolubility in water. Perfluorination of tris(pentafluorophenyl)borane and the pinacol units of the diborane molecule would make these molecules hydrophobic. It was reasoned that the adsorption capacity of G and the fact that the reaction is carried out in water would make these hydrophobic boron molecules to be adsorbed on the G sheet, hoping that they could act similarly as to whether a boron atom were inserted on G sheet. In support of this assumption, adsorption of BPh_3 on G was performed by refluxing of BPh_3 and G in the same proportion for 2 h and observing the presence of boron in XPS of the resulting G sample recovered by filtration (Figure S13). These all four boron-containing additives were added to undoped G in 1 wt. % that is in the

range of the amount of boron present in B-doped G (see Table 1).

The catalytic data showed that boron-containing organic molecules in these low amounts are able to enhance the activity of G, particularly boric acid and $(C_6F_5)_3B$. Figure 5 presents the time-yield plots for H_2 evolution for G and for G after adding these B-containing molecules. It can be seen there that the presence of these non-covalently bonded boron-containing molecules in such a low proportion increases significantly the catalytic activity of G for APR of glycerol. Although the activity of these additives enhanced the catalytic activity of G, the performance is still lower than that measured for (B)G. Therefore, the general strategy of adding boron compounds as additives to enhance the APR activity of G seems to be supported by the data presented in Figure 5. However, grafted boron atoms still exhibit higher activity. It is proposed that the beneficial activity of boron is related to the increase in the population of Lewis acid sites on the catalyst.
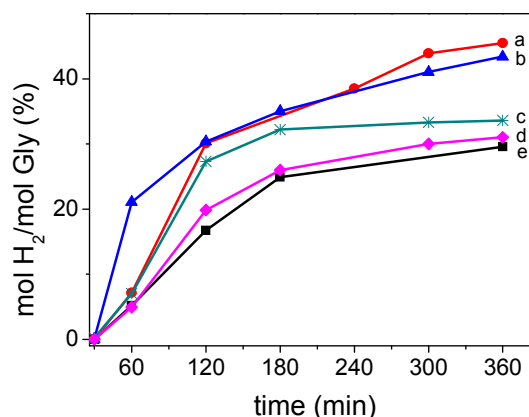

Figure 5. Temporal H_2 evolution in the APR of glycerol using G as catalyst in the absence (e) or in the presence of triphenylborane (a), boric acid (b) tris(pentafluorophenyl)borane (c) or bis(pinacolyl)diborane (d). Reaction conditions: Glycerol 10 vol. %, G 20 wt. % respect to glycerol, additive 1 wt. % respect G, temperature 250 ºC.

In order to gain some insight into the reaction mechanism the aqueous phase reaction was analysed at final reaction time to characterize the major components present in aqueous phase. It was observed that there was a residual concentration of glycerol still remaining in the aqueous phase at final reaction times, but many other products were also detected, including 1,3-propanediol derived from dehydroxylation of glycerol, 1-hydroxy-2-propanone and hydroxyacetone formed by dehydrogenation of glycerol, and acetoin (C_4) and ethyleneglycol (C_2), where the number of carbons has changed respect to that of glycerol. This distribution is in general agreement with reports in literature using metal catalyst for APR of glycerol.[17, 18]

Based on this product distribution, it seems that APR of glycerol has two major steps consisting in dehydrogenation of C-H bonds forming carbonyl groups and C-C bond breaking. It

is proposed that while dehydrogenation would be a catalytic process promoted by G, C-C bond cleavage of two neighbour carbonyl groups would occur spontaneously at the reaction temperature without the need of any catalyst due to the Coulombic repulsion between two positive neighbour carbon atoms in vic-dicarbonyl compounds decreasing the C-C bond energy. The following Scheme 2 illustrates this proposal.

In support of our mechanistic proposal, a control in the absence of G in aqueous medium at 250 $^{\circ}$C of oxalic acid shows its complete decomposition into H_2 and CO_2. Glyoxalic acid, having again in the structure two neighbour carbonyl groups, also decomposes in large extent forming H_2 and CO_2 in the gas phase in the absence of any catalyst. Thus, it seems that intermediates having two carbonyl groups next each other can decompose spontaneously at the reaction temperature as indicated in Scheme 2.

On the other hand, the hydrogenation activity of Gs has been recently reported and attributed to the presence of frustrated Lewis acid-base pairs.[14, 15] Thus, it seems that, as indicated in
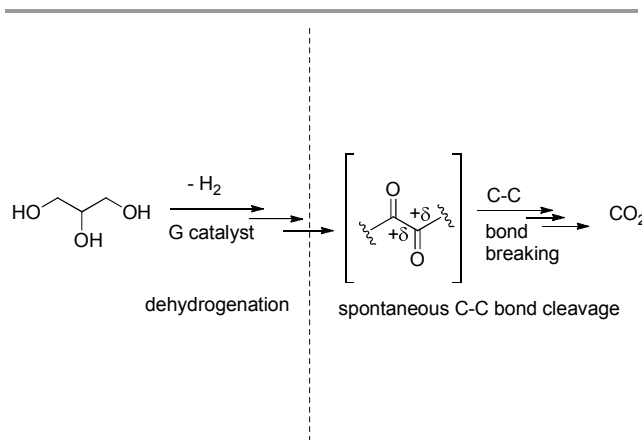
Scheme 2. Illustration of the two types of processes occurring in the APR of glycerol.

Scheme 2, the combination of the two processes should contribute to the observed activity of doped Gs in the APR of glycerol. The presence of B atoms on G would introduce Lewis acid sites that would be the limiting type of centre in the frustrated Lewis acid-base pairs in the present conditions. Carboxylate or other negatively charged oxygens present in G could act as basic sites. In this regard, the somewhat lower catalytic activity of co-doped (B,N)G vs. (B)G suggest that a higher population of basic sites can be even detrimental because it would reduce the density of frustrated Lewis acid-base pairs.

Conclusion

In the present study it has been shown that defective G materials obtained by pyrolysis of natural polysaccharides, particularly those containing B as dopant element, are active in the absence of any metal to promote the APR of glycerol at moderate temperatures. These findings are relevant in the

search for renewable and sustainable catalysts that could replace Pt as active metal in this reaction.

Experimental

Catalyst preparation.

Synthesis of doped G. The sodium salt from alginic acid and low molecular weight chitosan (Sigma Aldrich) were the precursors of G and (N)G respectively. These polysaccharides were pyrolyzed as powders under argon atmosphere using the following oven program: annealing at 200 $^{\circ}$C for 2 h and, then, heating at 10 $^{\circ}$C/min up to 900 $^{\circ}$C, maintaining this temperature for 6 h. The system was then cooled at room temperature under argon.

(B)G and (P)G were obtaining by dissolving 0.5 g of alginate in a boric acid (250 mg of HBO_3) or disodium hydrogen phosphate (1.6 g of Na_2HPO_4) aqueous solutions (50 ml), respectively. The solutions were, then, dried slowly by heating in an oven at 100 $^{\circ}$C overnight. The pyrolysis of these esters was performed using the same temperature program as that indicated above for the preparation of G and (N)G.

The same procedure was used to prepare (B,N)G, but using chitosan as precursor. In this way 0.5 g of chitosan was added to a boric acid aqueous solution (250 mg of HBO_3 in 25 ml of water). Acetic acid (0.45 g) was necessary for complete dissolution of chitosan. The solution was, then, dried slowly by heating in an oven at 100 $^{\circ}$C overnight. The pyrolysis was performed using the same oven program.

Suspensions of the corresponding G were obtained by sonicating at 700 W for 1 h in the aqueous glycerol solution the black solid graphitic residues obtained by pyrolysis until having a homogeneous dispersion. Remaining solid particles were removed by decantation.

Experimental procedure for the preparation of GO. Graphite flakes (3 g) were suspended in a mixture of concentrated H_2SO_4/H_3PO_4 (360:40 mL). To this mixture, $KMnO_4$ (18 g) was added by producing an exothermic reaction raising the temperature to 35-40 $^{\circ}$C. This reaction mixture was then heated to 50 $^{\circ}$C under stirring for 12 h. The reaction was cooled to room temperature and poured into 400 g of ice containing 30 % H_2O_2 (3 ml). After air cooling the suspension was filtered, washed with 1:10 HCl (37 %) solution and then further with water. The remaining solid was sonicated with 400 ml of water for 30 min and centrifuged at 4000 rpm for 4 h. The supernatant was centrifuged at 15000 rpm for 1h. The solid obtained after centrifugation at 15000 rpm was dried at 60 $^{\circ}$C.

General procedure for the APR reaction of glycerol.

The reaction was performed with a 2.5 mL aqueous solution 10% v/v of glycerol (3.43 mmol) in a stainless steel autoclave reactor (55 mL, Parker Autoclave Engineers). The autoclave apparatus allows sampling of the headspace gas of the reactor. The required amount of catalyst was added to the reaction mixture and the suspension sonicated before sealing the

Green Chemistry Accepted Manuscript

autoclave and heating at the corresponding temperature. The temporal evolution of the gas phase products was followed at the corresponding time by injecting 100 µL of the headspace gas in an Agilent 490 Micro-GC (Molsieve 5A column with Ar as a carrier gas). The Micro-GC has a precolumn filter to avoid injecting water from the reaction into the column. Product identification was made by their corresponding retention time, and the concentration was estimated from calibration data. At the end of the reaction the autoclave was cooled at room temperature and the liquid phase was analysed by HPLC (Waters 2410, Refractive index detector) with a column (ICE-COREGEL 87H3) using as eluent 0.004 M H_2SO_4 aqueous solution. Product identification was carried out based on their retention time compared to authentic commercial samples.

APR reaction of glucose.

The reaction was performed with a 2.5 mL aqueous solution of glucose (1.74 mmol) in a stainless steel autoclave reactor (55 mL, Parker Autoclave Engineers). Catalyst (20 wt. %) was added to the reaction mixture, and the system sealed and heated at 250 ^{o}C.

APR reaction of glycerol with G adding B-containing molecules.

The reaction was performed with a 2.5 mL aqueous solution 10% v/v of glycerol (3.43 mmol) in a stainless steel autoclave reactor (55 mL, Parker Autoclave Engineers). G catalyst (20 wt. %) and 1 wt. % of boron additive were added to the reaction mixture, and the system sealed and heated at 250 ^{o}C.

Physicochemical characterization.

Raman spectra (Renishaw in Via Raman Microscope) were carried out at room temperature with the 514.5 nm line of an Ar ion laser as excitation source.

Atomic force microscopy (AFM) measurements were made in air at ambient temperature with a Multimode Nanoscope 3A equipment working in tapping mode. It should be noted that AFM images were not acquired in a clean room.

TEM images were recorded in a JEOL JEM 2100F under accelerating voltage of 200 kV. Samples were prepared by applying one drop of the suspended material in ethanol onto a carbon-coated copper TEM grid, and allowing them to dry at room temperature.

XP spectra were recorded on a SPECS spectrometer equipped with a Phoibos 150 9MCD detector using a non-monochromatic X-ray source (Al and Mg) operating at 200 W. The samples were evacuated in the prechamber of the spectrometer at 1×10^{-9} mbar. The measured intensity ratios of components were obtained from the area of the corresponding peaks after nonlinear Shirley-type background subtraction and corrected by the transmission function of the spectrometer.

Acknowledgements.

Notes and References

1. R. D. Cortright, R. R. Davda and J. A. Dumesic, *Nature*, 2002, **418**, 964-967.
2. J. N. Chheda, G. W. Huber and J. A. Dumesic, *Angew. Chem. Int. Ed.*, 2007, **46**, 7164-7183.
3. J. Shabaker, G. Huber, R. Davda, R. Cortright and J. Dumesic, *Catalysis Letters*, 2003, **88**, 1-8.
4. G. W. Huber, J. W. Shabaker, S. T. Evans and J. A. Dumesic, *Applied Catalysis B: Environmental*, 2006, **62**, 226-235.
5. D. M. Alonso, S. G. Wettstein and J. A. Dumesic, *Chem. Soc. Rev.*, 2012, **41**, 8075-8098.
6. S. Navalon, A. Dhakshinamoorthy, M. Alvaro and H. Garcia, *Chemical Reviews*, 2014, **114**, 6179-6212.
7. J. Pyun, *Angewandte Chemie International Edition*, 2011, **50**, 46-48.
8. C. Su and K. P. Loh, *Accounts of Chemical Research*, 2013, **46**, 2275-2285.
9. A. Primo, P. Atienzar, E. Sanchez, J. Maria Delgado and H. Garcia, *Chemical Communications*, 2012, **48**, 9254-9256.
10. A. Primo, A. Forneli, A. Corma and H. García, *ChemSusChem*, 2012, **5**, 2207-2214.
11. D. R. Dreyer, H.-P. Jia and C. W. Bielawski, *Angewandte Chemie International Edition*, 2010, **49**, 6813-6816.
12. D. R. Dreyer, H.-P. Jia, A. D. Todd, J. Geng and C. W. Bielawski, *Organic & Biomolecular Chemistry*, 2011, **9**, 7292-7295.
13. A. Dhakshinamoorthy, A. Primo, P. Concepcion, M. Alvaro and H. Garcia, *Chemistry- A European Journal*, 2013, **19**, 7547-7554.
14. A. Primo, F. Neatu, M. Florea, V. Parvulescu and H. Garcia, *Nature Communications*, 2014, **5**.
15. M.-M. Trandafir, M. Florea, F. Neaţu, A. Primo, V. I. Parvulescu and H. García, *Chemsuschem*, 2016, **9**, 1565-1569.
16. A. Primo, V. Parvulescu and H. Garcia, *Journal of Physical Chemistry Letters*, 2017, **8**, 264-278.
17. J. C. Thompson and B. B. He, *Applied Engineering in Agriculture*, 2006, **22**, 261-265.
18. G. Wen, Y. Xu, H. Ma, Z. Xu and Z. Tian, *international journal of hydrogen energy*, 2008, **33**, 6657-6666.
19. W. S. Hummers and R. E. Offeman, *Journal of the American Chemical Society*, 1958, **80**, 1339-1339.
20. S. Stankovich, D. A. Dikin, R. D. Piner, K. A. Kohlhaas, A. Kleinhammes, Y. Jia, Y. Wu, S. T. Nguyen and R. S. Ruoff, *Carbon*, 2007, **45**, 1558-1565.
21. M. Latorre-Sánchez, A. Primo and H. García, *Angew. Chem. Int. Ed.*, 2013, **52**, 11813-11816.
22. Z.-H. Sheng, H.-L. Gao, W.-J. Bao, F.-B. Wang and X.-H. Xia, *Journal of Materials Chemistry*, 2012, **22**, 390-395.
23. H. Wang, Y. Zhou, D. Wu, L. Liao, S. Zhao, H. Peng and Z. Liu, *Small*, 2013, **9**, 1316-1320.
24. J. Long, X. Xie, J. Xu, Q. Gu, L. Chen and X. Wang, *ACS Catalysis*, 2012, **2**, 622-631.

Please do not adjust margins
Green Chemistry

ARTICLE

25. J.-H. Yang, G. Sun, Y. Gao, H. Zhao, P. Tang, J. Tan, A.-H. Lu and D. Ma, *Energy & Environmental Science*, 2013, **6**, 793-798.
26. W. Wei and G. Jinlong, *Frontiers of Chemical Science and Engineering*, 2011, **5**, 2-10.
27. R. R. Davda, J. W. Shabaker, G. W. Huber, R. D. Cortright and J. A. Dumesic, *Appl. Catal., B*, 2003, **43**, 13-26.
28. R. R. Davda, J. W. Shabaker, G. W. Huber, R. D. Cortright and J. A. Dumesic, *Appl. Catal., B*, 2005, **56**, 171-186.

Green Chemistry Accepted Manuscript